Influence of crystal size and probe molecule on diffusion in hierarchical ZSM-5 zeolites prepared by desilication

Author(s):
Meunier, Frederic C.; Verboekend, Danny; Gilson, Jean-Pierre; Groen, Johan C.; Pérez-Ramírez, Javier

Publication Date:
2012-01-15

Permanent Link:

https://doi.org/10.3929/ethz-a-010788848 →

Originally published in:

Microporous and Mesoporous Materials 148(1), http://doi.org/10.1016/j.micromeso.2011.08.002 →

Influence of crystal size and probe molecule on diffusion in hierarchical ZSM-5 zeolites prepared by desilication

Frederic C. Meunier*[a], Danny Verboekend[b], Jean-Pierre Gilson[a], Johan C. Groen[c] and Javier Pérez-Ramírez*[b]

[a] *Laboratoire Catalyse et Spectrochimie, ENSICAEN, University of Caen, CNRS, 6 Bd Maréchal Juin, 14050, Caen, France.*

[b] *Institute for Chemical and Bioengineering, Department of Chemistry and Applied Biosciences, ETH Zurich, Wolfgang-Pauli-Strasse 10, HCI E 125, CH-8093, Zurich, Switzerland.*

[c] *Delft Solids Solutions, B.V., Rotterdamseweg 183C, 2629 HD Delft, The Netherlands.*

* Corresponding authors: E-mail (FCM): frederic.meunier@ensicaen.fr; E-mail (JPR): jpr@chem.ethz.ch

Address for correspondence:
Dr Frederic C. Meunier
Laboratoire Catalyse et Spectrochimie
CNRS - University of Caen - ENSICAEN
6 Boulevard du Marechal Juin
14050 Caen Cedex, France
Phone: + 33 (0) 231452731
Fax: +33 (0) 231452822
E-mail: frederic.meunier@ensicaen.fr

Abstract

The improvement of molecular transport properties of hierarchical H-ZSM-5 obtained by desilication was evidenced by studying the desorption of *o*-xylene and isooctane by *in situ* diffuse reflectance infrared Fourier transform spectroscopy (DRIFTS). This technique enabled monitoring simultaneously bands associated with the molecular probes and the zeolite, using powdered sample masses as low as 1 mg. Two H-ZSM-5 samples with markedly different crystal sizes and shapes were investigated. The first sample was commercial and consisted of small crystallites (*ca*. 250 nm). The second sample were laboratory-made large crystals with coffin-like shape (*ca.* 17×4×4 μm^3). The hierarchical derivatives of the small and large zeolite crystals displayed 250 and 120 $m^2 g^{-1}$ of mesopore surface area, respectively, in contrast to the 62 and 5 $m^2 g^{-1}$ of the parent counterparts. The data based on *o*-xylene desorption were partly disguised by site-desorption limitations. Desorption experiments using isooctane evidenced a 4-fold reduction in the characteristic diffusion path length on both mesoporous small and large zeolites with respect to their purely microporous analogues. These results confirm the substantial potential for improvement of commercial nanocrystalline zeolites in diffusion-limited reactions upon the introduction of intra-crystalline mesoporosity by post-synthesis modification.

Keywords: Hierarchical zeolites; H-ZSM-5; Desilication; Diffusion; Isooctane; *o*-xylene; Infrared spectroscopy.

1. Introduction

Zeolites are microporous aluminosilicates extensively applied in industrial catalytic and adsorption/separation processes [1,2]. The intrinsic microporosity of these solids often imposes molecular diffusion limitations due to hindered access and slow intra-crystalline transport. This leads to a substantial under-utilization of the potential of zeolites in catalytic applications by limiting the corresponding activity, selectivity, and catalyst lifetime [3]. Hierarchical (or mesoporous) zeolites can alleviate these issues by adding to the native microporosity an auxiliary network of inter- and/or intra-crystalline mesopores. The added mesoporosity increases the number of accessible micropores and effectively shortens the average path length to the active sites, hereby increasing their catalytic performance [4-7]. A wide variety of methods are available to prepare mesoporous zeolites [4,8-11]; those involve either the alteration of the synthesis protocol (bottom-up) or the post-synthetic modification of conventionally prepared zeolites (top-down). Controlled silicon leaching in alkaline media, known as desilication, belongs to the latter category and is widely applied due to a combination of simplicity, versatility, and efficiency [12,13].

Beneficial effects of hierarchical zeolites have been reported for a wide range of catalyzed reactions and often assigned automatically to improved transport or reduced diffusion constraints. However, the number of studies additionally reporting diffusion data is rather limited [4,7]. One should therefore carefully consider whether the catalytic benefits in hierarchical zeolites can be solely attributed to the introduction of mesoporosity, since other parameters such as the chemical composition, the acid site distribution or the number of defects may be also affected in the mesopore formation process [13-17]. As a matter of fact, Kortunov *et al.* [18] studied the diffusion of *n*-

72 octane and 1,3,5-triisopropylbenzene in zeolite Y and the mesoporous derivative
73 prepared by steaming [5] (ultra-stable Y, USY) and concluded that, in this particular
74 case, steaming did not significantly affect intra-crystalline diffusion probably because
75 the created mesopores were not interconnected with the native micropores. De Jong and
76 co-workers had earlier shown by 3D-TEM analysis that mesopores were occluded
77 within the USY crystals and not accessible from the external surface [19].

78 Improved diffusion properties have been reported in the case of hierarchical zeolites
79 with *interconnected* mesopores. Groen *et al.* [20] and Zhao *et al.* [21] measured the rates
80 of uptake of neopentane and cumene, respectively, in microporous and hierarchical
81 ZSM-5 zeolites. Both authors reported uptake rates 2-3 orders of magnitude higher for
82 the hierarchical samples. Cho *et al.* [22] measured the uptake of Xe in hierarchical LTA
83 zeolites and showed that the diffusivity increased linearly with the degree of
84 mesoporosity in the samples. Other studies [23-26] have also reported increased
85 desorption rates of probe molecules (isobutane, neopentane, butane, and propane) over
86 hierarchical zeolites versus conventional zeolites.

87 Diffusion studies have traditionally focused on purely microporous and carefully
88 grown (large) crystals [27-31]. Yet, small crystals (<1 μm) should be also used to
89 establish that improved transport could be attained on industrially relevant zeolites. To
90 our knowledge, no direct comparison of the improvements in the transport property
91 upon introduction of mesoporosity is available for both large and small (commercial)
92 zeolite crystals of the same structure.

93 The present work reports an investigation on the diffusion in hierarchical zeolites of
94 very different crystal sizes obtained by desilication. ZSM-5 was primarily selected
95 because of its relevance in industrial catalysis [2]. Small (<1 μm diameter, noted “SP”)

and large (17×4×4 μm^3, noted "LP") ZSM-5 crystals and the hierarchical derivatives obtained by alkaline treatment (noted "SAT" and "LAT", respectively) were investigated. Examining both small and large crystals is worthwhile because large crystals are often used as model systems exhibiting reasonably well-defined geometric forms and sizes, while small crystals are of more practical importance. The specific parent and alkaline-treated zeolite samples have been extensively characterized in previous studies [16,20]. The desorption of *o*-xylene and isooctane (*i.e.* 2,2,4-trimethylpentane, also noted iC8), which both exhibit a kinetic diameter larger than the H-ZSM-5 pore size, was monitored. This approach may limit the influence pore entrance effects as described by Reitmeier *et al.* [32] and make the diffusion of the sorbate through the pores the transport-limiting step, leading to an unambiguous assessment of the improvement related to the introduction of mesoporosity.

2. Experimental

2.1. Materials and characterization

The parent small crystals (SP) were obtained by calcination of a commercial NH_4-ZSM-5 (Zeolyst, CBV 8014, measured Si/Al ratio = 47) in static air at 823 K for 5 h using a heating rate of 5 K min^{-1}. The corresponding hierarchical H-ZSM-5 sample (SAT) was obtained by an alkaline treatment in 0.2 M of NaOH at 338 K for 30 min, followed by three consecutive ion exchanges in 0.1 M NH_4NO_3 and calcination [16]. The large ZSM-5 crystals (LP), featuring a Si/Al = 30, were synthesized as described elsewhere [20]. Applying the recipe given in this reference, the hierarchical sample (LAT) was prepared by an alkaline treatment in 0.2 M of NaOH at 338 K for 120 min, followed by ion exchange with NH_4NO_3 and calcination.

120 The Si and Al content in the solids were determined by inductively coupled plasma
121 optical emission spectroscopy (ICP-OES) (Perkin-Elmer Optima 3200RL (radial)). N_2
122 isotherms at 77 K were measured with a Quantachrome Quadrasorb-SI gas adsorption
123 analyser. Prior to the measurement, the samples were degassed in vacuum at 573 K for
124 10 h. The *t*-plot method was used to discriminate between micro- and mesoporosity
125 [33]. The Brunauer-Emmett-Teller (BET) method [34] was applied to determine the
126 total surface area (S_{BET}), which is used for comparative purposes. The pore size
127 distribution (PSD) was obtained by applying the Barret-Joyner-Halenda (BJH) model
128 [35] to the adsorption branch of the isotherm.
129

130 **2.2. Desorption measurements**

131 Between 1 and 5 mg of zeolite powder was deposited onto a SiC bed in the crucible of a
132 high temperature-low pressure diffuse reflectance FTIR spectroscopy (DRIFTS)
133 reaction cell from Spectra-Tech. The cell was placed in a Collector assembly from
134 Spectra-Tech and fitted in a Nicolet Magna 550 FTIR spectrometer equipped with a
135 MCT detector cooled with liquid nitrogen. A FTIR spectrum recorded over SiC was
136 used as background. The DRIFTS spectra of the zeolites were plotted as log 1/R, where
137 R is the sample reflectance. The function log 1/R (= pseudo-absorbance) provides better
138 linearity between band intensity against coverage than that given by the Kubelka-Munk
139 function for strongly absorbing media, such as those based on oxides [36].
140 The reaction cell was modified to eliminate bed by-pass by inserting some PTFE tape
141 between the ceramic crucible and the metallic base plate. The only difference with the
142 cell modifications described in [37] is that a quartz wool plug was used in place of a
143 metallic mesh to hold the sample bed. High-purity Ar or CO from Air Liquide was fed

144 through low-volume heated stainless-steel lines to the cell and through saturators kept at
145 273 K to carry the vapor of the hydrocarbons. The samples were initially equilibrated
146 under 1.0 vol.% isooctane or 0.18 vol.% *o*-xylene in Ar at 423 K.

147 The contribution of gas-phase hydrocarbons to the DRIFTS signal was determined
148 from reference experiments using CO (an IR-sensitive gas) as the carrier gas. The gas-
149 phase spectrum of CO and the hydrocarbon mixture was measured at the exit of the
150 DRIFTS cell in a transmission FTIR gas-cell (optical path length: 27 cm) and was
151 thereafter used to eliminate gas-phase signals from the overall DRIFTS signal. The
152 contribution of the gas-phase signal of the hydrocarbon probes on the overall DRIFTS
153 band intensity was shown to be lower than 10% in all cases.

154 A gas flow rate of 60 cm^3 STP min^{-1} of pure Ar was used to purge the hydrocarbon
155 from the system during the desorption experiment. No differences in desorption rates
156 were noted when flow rates ranging between 30 and 120 cm^3 STP min^{-1} were used. The
157 time-resolved desorption of hydrocarbons was monitored and the relative surface
158 concentration of the hydrocarbons was calculated using the IR bands corresponding to
159 the C-H stretching vibrations (integrated over 3020-2800 cm^{-1} and 3001-2848 cm^{-1} for
160 isooctane and *o*-xylene, respectively) normalized to the zeolite overtone bands
161 (integrated over 2100-1800 cm^{-1}). The spectra were recorded with a resolution of 4 cm^{-1}
162 and an accumulation of 4 scans initially every 4 seconds following the removal of the
163 hydrocarbons. The IR spectra were analyzed using the OMNIC software. The initial
164 slope of the normalized decaying IR band intensity plotted against the square root of
165 time was used to determine the modification in the characteristic diffusion length of the
166 samples (*vide infra*).

167 The sorbate concentrations in the zeolites were derived from calibration curves

168 measured over the same materials using an *in situ* quartz transmission IR cell fitted with
169 KBr windows. This was achieved by carrying out titration-type experiments at room
170 temperature over a zeolite wafer of known weight. The samples were first evacuated
171 under secondary vacuum ($P < 10^{-5}$ torr) at 523 K for 15 min. The hydrocarbon signal
172 normalized to the zeolite overtones bands (*vide infra*) was then monitored as a function
173 of the number of calibrated pulses sent into the cell. The number of moles in each pulse
174 was determined from the known volume of the injection chamber (1.73 cm^3) and the
175 pressure in the injection lines read on a Pfeiffer pressure gauge.
176
177 **2.3. Calculation of characteristic diffusion lengths and diffusivities**
178 The desorption curves plotted as a function of the square root of time were used to
179 calculate the (non-steady-state) diffusivity D_{ns} [38,39]. The expression of D_{ns} is given
180 by equation 1:
181
182 $$D_{ns} = \frac{\pi}{4} \cdot L^2 . slope^2 \qquad \text{(eqn. 1)},$$
183 where L is the characteristic diffusion length of the crystallite and "slope" is the initial
184 slope of the desorption curve plotted as a function of the square root of time [20,40].
185 The characteristic diffusion length is usually taken as the ratio between the volume and
186 external surface of the crystallite and is equal, in the case of a spherical particle, to a
187 third of the particle radius r, so that eqn. 1 rearranges to:
188
189 $$D_{ns} = \frac{\pi}{36} \cdot r^2 . slope^2 \qquad \text{(eqn. 2)}.$$
190
191 Note that these equations are equivalent to those reported by Muller *et al.* [30] and

Groen *et al.* [20]. These D_{ns} values are marred by the accumulation of hydrocarbons in the sample, leading to the presence of effectively "immobile" molecules alongside the mobile species [38]. The D_{ns} values must be corrected by an accumulation factor h [38] to determine the steady-state diffusivity D_{ss}:

$$D_{ss} = h\, D_{ns} = \frac{C_T}{C_0} D_{ns} \qquad \text{(eqn. 3)},$$

where C_T (mol m^{-3}) is the total concentration of hydrocarbon in the zeolite and C_0 (mol m^{-3}) is the corresponding gas-phase concentration. Considering the sorbate as an ideal gas:

$$C_0 = \frac{P}{R\,T} \qquad \text{(eqn. 4)},$$

where P (Pa) is the partial pressure of the sorbate, R = 8.314 J K^{-1} mol^{-1}, and T (K) is the adsorption temperature. C_T was determined *via* calibration curves as described in the previous section.

The slope and the corresponding apparent D_{ss} values of the hierarchical H-ZSM-5 crystals (calculated assuming the same crystallite size or characteristic diffusion length, L) were significantly higher than those of the parent samples. It was yet assumed that the true D_{ss} was constant and that the experimental differences only arose from a decreased size or characteristic diffusion length. The effective size and L values were therefore computed by imposing the same D_{ss} as that measured on the parent crystals.

3. Results

3.1. Zeolites

The SP sample with Si/Al = 47 consisted of 2-3 μm agglomerates made of *ca.* 250 nm primary spherical crystallites (average size determined by TEM, data not shown). The LP sample with Si/Al = 30 consisted of large (*ca.* 17×4×4 μm^3) ZSM-5 crystals with coffin-like shape. Microscopy studies and further characterization of the starting zeolites can be found elsewhere (small crystals in [16] and large crystals in [20]). Treatment of ZSM-5 zeolites with Si/Al=25-50 in aqueous NaOH solutions under the conditions used in this work (0.2 M, 338 K, 30-120 min) is known to generate extensive intracrystalline mesoporosity in the zeolites by selective extraction of framework silicon [41,42]. Due to this, the molar Si/Al ratio of the samples decreased (Table 1). The development of mesoporosity is clearly observed by gas adsorption. Fig. 1 shows that the typical type I N_2 isotherm in the purely microporous sample transforms into a combined I and IV isotherm in the NaOH-treated sample, a known fingerprint of a hierarchical porous system [4]. The hierarchical derivatives of the small and large zeolite crystals displayed a mesopore surface area (S_{meso}) of 250 and 120 $m^2\,g^{-1}$, respectively, in contrast to the values of 62 and 5 $m^2\,g^{-1}$ for the parent counterparts (Table 1). As commonly reported, the hierarchical zeolites displayed an increased total pore volume (V_{pore}) and total surface area (S_{BET}), while the micropore volume (V_{micro}) decreased. The mesopore size distribution was centered around 10 nm in both hierarchical samples (insets of Fig. 1). Additional characterization of these specific alkaline-treated zeolites [16,20] is not elaborated here for the sake of conciseness. We can briefly highlight that the alkaline-treated samples maintain the long-range crystallinity of the parent zeolites (determined by X-ray diffraction) as well as the

original micropore size (determined by high-resolution low-pressure Ar adsorption at 87 K). Mercury porosimetry indicated that the 10 nm mesopores are accessible from the external surface of the crystal, that is, desilication does not generate occluded mesoporosity. In addition, the acidity properties (NH_3-TPD and infrared of pyridine and/or CO adsorbed) are largely preserved.

3.2. Diffusion measurements

The *in situ* DRIFTS spectra of the activated SP and SAT samples equilibrated under pure Ar, 178 Pa of *o*-xylene or 1 kPa of isooctane are shown in Figs. 2a-b. The alkaline-treated sample exhibited a markedly higher proportion of terminal silanol groups (*ca.* 3740 cm^{-1}), due to the higher external surface of this sample created by desilication. The adsorption of *o*-xylene (Fig. 2a) on both the SP and SAT materials was significantly stronger than that of isooctane (Fig. 2b), as evidenced by the significant decrease of the bridged hydroxyls band at 3600 cm^{-1} and the concomitant formation of H-bonded hydroxyls (broad band over 3600-3000 cm^{-1}) observed in the case of *o*-xylene.

The rates of desorption of *o*-xylene and isooctane from SP and SAT were assessed. The desorption rate of *o*-xylene marginally increased in the case of SAT as compared to that of SP (Fig. 3, top). The corresponding characteristic diffusion length decreased by a factor 1.4 (calculated using an average crystal diameter of 250 nm for the parent zeolite). However, the improvement in desorption rate was markedly higher in the case of isooctane (Fig. 3, bottom), leading to a 3.6-fold shorter characteristic diffusion length.

This apparent discrepancy between the transport improvements of *o*-xylene and isooctane was rationalized by calculating the characteristic desorption time of these

molecules from the surface sites using elementary kinetic theory [38]. Assuming sorption heats on H-ZSM-5 for *o*-xylene and isooctane of 120 and 100 kJ mol^{-1} [43,44], respectively, the corresponding desorption times should be about 65 s and less than 0.2 s at 428 K. This indicates that *o*-xylene removal from the crystals was limited by both (i) the stochastic diffusion (Fickian) process and (ii) a site-desorption controlled molecular transport, while the latter constraint was negligible in the case of isooctane. Therefore, *only* the isooctane data can be used to determine the true decrease in characteristic diffusion length under the present experimental conditions.

The desorption of isooctane was also followed over the large H-ZSM-5 crystals. Similarly to the case of the SP and SAT (Fig. 2b), iC8 only interacted weakly with the Brønsted acid sites of LP and LAT (Fig. 2c). The desorption time of isooctane was markedly shorter over LAT than over LP (Fig. 4). The corresponding apparent decrease in characteristic diffusion length was about 3.9 (calculated using an average characteristic diffusion length of 0.8 μm for the parent zeolite [20]).

It must be stressed that the isooctane concentration in SP, SAT, LP, and LAT were similar (Fig. 5). Therefore a similar amount of sorbate was removed in each case, allowing a direct comparison of the slope of the linear part of the desorption curves [45]. The initial desorption rate over LAT was similar or even faster than that observed over SP, indicating that the transport of sorbate in the mesoporous large crystal resembled that in the parent commercial H-ZSM-5. Note that the differences in the shape of the desorption curves were due to the fact that a different distribution of characteristic lengths were present in each case, making a detailed calculation of characteristic diffusion path length very difficult.

4. Discussion

The present data highlights a remarkable improvement of the desorption rates of *o*-xylene and, even more clearly, of isooctane (Fig. 3) on hierarchical H-ZSM-5 obtained by controlled silicon dissolution in alkaline medium. The transport improvement was evidenced for both small commercial crystals and large H-ZSM-5 crystals (Fig. 4).

While the nature of the sorbate and the experimental conditions can affect the nature of the step limiting the transport (*vide infra*), the crystallite size can also be determining. It has been proposed that intra-crystalline diffusion was limiting the uptake of benzene, toluene, and *p*-xylene over 3-4 µm ZSM-5 particles, while the uptake was controlled by surface barriers for particles smaller than 100 nm [46]. These observations stress the difficulty to compare data from various systems.

It must be noted that the *in situ* DRIFTS data collected in the present study were reproducible. The error on the value of the slope of the decaying signal of the desorbing hydrocarbon was found to be below 10%. In summary, DRIFTS is a convenient investigative technique because it enables:

i. directly using a powder, and not a pressed wafer, in which additional transport limitation may occur,
ii. using sample masses as low as 1 mg and a high flow rate of purge gas, which limit inter-crystalline re-adsorption
iii. monitoring simultaneously bands associated with the probes (gas phase and adsorbed) and with the zeolite, allowing quantitative analyses.

DRIFTS band intensities are essentially proportional to sorbate concentrations, providing pseudo-absorbance (and not Kubelka-Munk) units are used when sorbate reflectance is high, as is typically the case in studies pertaining to heterogeneous

311 catalysts [36]. A limitation of DRIFTS is that only a fraction of the bed is probed [47];
312 this becomes negligible when sample beds are homogeneous and inter-crystalline re-
313 adsorption is reduced by using very low sample amounts and high purge gas flow rate
314 as in the present study.

315 The signal-to-noise ratio of the DRIFTS-based plots (Figs. 3 and 4) were clearly
316 lower than that obtained for instance on a TEOM microbalance as described in [20].
317 This is a compromise that is usually acceptable, taken into account the cost and
318 availability of DRIFTS equipment and the ease with which the data can be obtained.
319 The lower accuracy of DRIFTS-based measurements could also explain the somewhat
320 lower uptake of isooctane observed over SAT as compared to SP, LP and LAT (Fig. 5),
321 although isooctane adsorption isotherms should be measured to ascertain this point.

322 Diffusion studies carried out using different methods and experimental conditions
323 have often led to diffusivity values varying by orders of magnitude [38,39,48]. Some of
324 these discrepancies arise from confusions in the description of the state of the molecules
325 present in the sorbent, a fraction (determined by thermodynamics) being immobilized,
326 while the remaining part effectively participates to the molecular transport (with a given
327 diffusivity D_{ss}) at any given time [38]. This problem is solved by correcting the apparent
328 non-steady-state diffusivity D_{ns} with the accumulation factor to obtain the D_{ss} as
329 described in the experimental section [38,39].

330 The desorption of *o*-xylene (kinetic diameter = 0.74 nm) and isooctane (kinetic
331 diameter = 0.62 nm) was used in the present study. These molecules were chosen
332 because those exhibit kinetic diameters larger than the crystallographic pore size of H-
333 ZSM-5 (*ca.* 0.56 nm) and should make molecular transport through the MFI micropores
334 the rate-determining step.

Another difficulty plaguing diffusivity measurements is that the step limiting the transport may depend on the sorbate and experimental conditions. The comparison of the desorption curves of *o*-xylene and isooctane over SP and SAT (Fig. 3) and the associated characteristic desorption times [38] clearly evidenced such occurrence in the present case. The interaction of *o*-xylene was sufficiently strong with the Brønsted acid sites of the H-ZSM-5 (as evidenced by the formation of a large H-bonded hydroxyl band, Fig. 2.a) so that the site desorption time became significant (*ca.* 65 s) in comparison to the timescale of the desorption experiment (more than 80% of *o*-xylene desorbed within 7 min). The benefit of mesoporosity in the SAT sample was therefore limited, since the stochastic diffusion process throughout the hierarchical pore system became less dominant. Consequently, probe molecule selection is a vital aspect to measure true diffusion properties in zeolites.

The steady-state diffusivity of *o*-xylene calculated assuming a crystallite diameter for SP of 250 nm was D_{ss} (SP, average crystal size 250 nm) = 1.8×10^{-10} cm^2 s^{-1}. This value is slightly smaller than that reported for highly siliceous H-ZSM-5 over identical experimental conditions [39], *i.e.* D_{ss} = 2.5×10^{-10} cm^2 s^{-1}. A lower apparent value of steady-state diffusivity for *o*-xylene was expected here, because of the higher acid site concentration of our samples that slowed down the diffusion of the sorbate.

The steady-state diffusivity of isooctane at 428 K calculated assuming a crystallite diameter for SP of 250 nm was D_{ss} (SP, 250 nm) = 2.4×10^{-12} cm^2 s^{-1}, while the value calculated for the same molecule over the LP H-ZSM-5, assuming a characteristic diffusion length of 800 nm [20] was D_{ss} (LP, L = 800 nm) = 77×10^{-12} cm^2 s^{-1}. These values are expected to be equal and the 32-fold higher diffusivity measured for LP suggests that the average small crystal size and/or the characteristic diffusion length of

359 the large crystal were badly estimated. We are not aware of any work reporting
360 isooctane diffusivity values over H-ZSM-5 under similar experimental conditions that
361 could help resolve this matter.

362 It is most likely that the characteristic diffusion length of the large crystal was much
363 smaller. A close analysis of the micrographs reported in [20] indicates that LP did not
364 consist of single crystals but the particles were formed of intergrown units. One can
365 therefore propose that the defects at the intergrowth could offer a low resistance to
366 isooctane transport. Assuming that the true diffusivity of isooctane in H-ZSM-5 at
367 428 K was that measured in SP, *i.e.* D_{ss} = 2.4×10^{-12} cm^2 s^{-1}, then the effective
368 characteristic diffusion length of LP should be 140 nm (and not 800 nm).

369 Note that the characteristic diffusion length of a sphere is a third of its radius and
370 therefore L = 42 nm for SP (250 nm). The characteristic lengths of SP and LP would
371 therefore amount to 42 and 140 nm, respectively. Whatever the true characteristic
372 diffusion length of LP, the improvement of isooctane transport observed in the LAT
373 remains the same and corresponds to a *ca.* 4-fold decrease of the diffusion path length.

374 The similar decrease of characteristic diffusion length observed over the small and
375 large hierarchical crystals, *i.e.* factors 3.6 and 3.9, respectively, implied major structural
376 changes. A more than 50-fold decrease of the volume of the effective elementary
377 crystallite was achieved in the present case. The possibility to create mesoporous
378 zeolites especially from small crystals by post-synthetic alkaline treatments is a major
379 asset and further confirms the suitability of desilication for improving molecular
380 transport over commercial catalysts.

381 In the work by Groen *et al.* [20] over the same LP and LAT H-ZSM-5 crystals, a 10-
382 fold decrease of the characteristic diffusion path length was noted for about 50% of the

crystals. This is higher than our present observation over the same materials, *i.e.* an overall 4-fold decrease was observed. This discrepancy could be due to the differing experimental method (adsorption uptake in a TEOM microbalance) and probe molecule (neopentane). Moreover, no attempt was made here to deconvolute the decay signal because of the lower signal-to-noise ratio obtained with our IR based-data. This is also a reminder that the mesoporosity creation by desilication may not always be homogeneous through the zeolite, as described by Groen *et al.* [20].

Overall, our results support the view that the improved catalytic performance over commercial mesoporous zeolites [4,7] is largely due to improved transport, which has been unambiguously quantified in our study. Diffusion studies on large crystals can also have a practical relevance and serve as a guide, despite being model systems. Large zeolite crystals may sometimes offer the advantage of presenting better-defined sizes and shapes, although the presence of intergrowth should not be neglected and could decrease the actual characteristic diffusion length.

In addition, the characteristic diffusion lengths of reactants in hierarchical zeolites and their parents leads to an easy and quantitative measurement of the associated catalytic improvements when single file diffusion is not dominant [49-52], *i.e.* where the Thiele modulus can be used.

5. Conclusions

The present work demonstrates that a combination of DRIFTS and transmission FTIR can deliver accurate quantitative diffusivity values in a simple, cost-effective, and fast manner. The choice of the probe and experimental conditions are critical if the transport properties are to be free of site-desorption effects, as observed here in the case of *o*-

xylene. In the case of isooctane, a *ca.* 4-fold reduction in the characteristic diffusion path length of both submicron and large H-ZSM-5 crystals was observed. These results show that desilication is a highly efficient synthetic strategy to alleviate diffusion limitations in commercial zeolite catalysts (typically submicron crystals) by producing hierarchical samples to an extent comparable to that observed in the desilication of (model) large crystals.

Acknowledgements

ETH Zurich, the Swiss Science National Foundation (project number 200021-134572), the ANR (Hizecoke project, 2010 BLAN 723), and the Région Basse-Normandie are acknowledged for financial support.

References

[1] A. Corma, Chem. Rev., 95 (1995) 559.

[2] W. Vermeiren, J.-P. Gilson, Top. Catal., 52 (2009) 1131.

[3] A. Corma, Chem. Rev., 97 (1997) 2373.

[4] J. Pérez-Ramírez, C.H. Christensen, K. Egeblad, C.H. Christensen, J. C. Groen, Chem. Soc. Rev., 37 (2008) 2530.

[5] S. van Donk, A.H. Janssen, J.H. Bitter, K. P. de Jong, Catal. Rev. -Sci. Eng., 45 (2003) 297.

[6] R. Chal, C. Gerardin, M. Bulut, S. van Donk, ChemCatChem, 3 (2011) 67.

[7] M.S. Holm, E. Taarning, K. Egeblad, C.H. Christensen, Catal. Today, 168 (2011) 3.

[8] L. Tosheva, V. Valtchev, Chem. Mater., 17 (2005) 2494.

[9] W.J. Roth, J. Čejka, Catal. Sci. Technol., 1 (2011) 43.

[10] J. Čejka, S. Mintova, Catal. Rev. -Sci. Eng., 49 (2007) 457.

[11] K. Egeblad, C.H. Christensen, M. Yu. Kustova, C. H. Christensen, Chem. Mater., 20 (2008) 946.

[12] J. C. Groen, L.A.A. Peffer, J.A. Moulijn, J. Pérez-Ramírez, J. Mater. Chem., 16 (2006) 2121.

[13] D. Verboekend and J. Pérez-Ramírez, Catal. Sci. Technol., 2011, doi: 10.1039/C1CY00150G.

[14] M.S. Holm, S. Svelle, F. Joensen, P. Beato, C.H. Christensen, S. Bordiga, M. Bjørgen, Appl. Catal. A: Gen., 356 (2009) 23.

[15] F. Thibault-Starzyk, I. Stan, S. Abelló, A. Bonilla, K. Thomas, C. Fernandez, J.-P. Gilson, J. Pérez-Ramírez, J. Catal., 264 (2009) 11.

[16] C. Fernandez, I. Stan, J.-P. Gilson, K. Thomas, A. Vicente, A. Bonilla and J. Pérez-Ramírez, Chem. Eur. J., 16 (2010) 6224.

[17] P. Sazama, B. Wichterlova, J. Dedecek, Z. Tvaruzkova, Z. Musilova, L. Palumbo, S. Sklenak, O. Gonsiorova, Microporous Mesoporous Mater., 143 (2011) 87.

[18] P. Kortunov, S. Vasenkov, J. Kärger, R. Valiullin, P. Gottschalk, M. F. Elía, M. Perez, M. Stöcker, B. Drescher, G. McElhiney, C. Berger, R. Gläser, J. Weitkamp, J. Am. Chem. Soc., 127 (2005) 13055.

[19] A.H. Janssen, A.J. Koster, K.P. de Jong, Ang. Chem. Int. Ed., 40 (2001) 1102.

[20] J.C. Groen, W. Zhu, S. Brouwer, S.J. Huynink, F. Kapteijn, J.A. Moulijn, J. Pérez-Ramírez, J. Am. Chem. Soc., 129 (2007) 355.

[21] L. Zhao, B. Shen, J. Gao, J. Gao, C. Xu, J. Catal., 258 (2008) 228.

[22] K. Cho, H.S. Cho, L.-C. de Menorval, R. Ryoo, Chem. Mater., 21 (2009) 5664.

[23] C.H. Christensen, K. Johannsen, E. Törnqvist, I. Schmidt, H. Tøpsoe, C.H. Christensen, Catal. Today, 128 (2007) 117.

[24] J. Pérez-Ramírez, D. Verboekend, A. Bonilla, S. Abelló, Adv. Funct. Mater., 19 (2009) 3972.

[25] D. Verboekend, J.C. Groen, J. Pérez-Ramírez, Adv. Funct. Mater., 20 (2010) 1441.

[26] D. Verboekend, R. Caicedo-Realpe, A. Bonilla, M. Santiago, J. Pérez-Ramírez, Chem. Mater., 22 (2010) 4679.

[27] L. Zhang, C. Chmelik, A.N.C. van Laak, J. Kärger, P.E. de Jongh, K.P. de Jong, Chem. Commun., (2009) 6424.

[28] P. Kortunov, C. Chmelik, J. Kärger, R.A. Rakoczy, D.M. Ruthven, Y. Traa, S. Vasenkov, J. Weitkamp, Adsorption, 11 (2005) 235.

[29] P. Kortunov, S. Vasenkov, C. Chmelik, J. Kärger, D.M. Ruthven, J. Wloch, Chem. Mater., 16 (2004) 3552.

[30] G. Muller, T. Narbeshuber, G. Mirth, J.A. Lercher, J. Phys. Chem., 98 (1994) 7436.

[31] M.H.F. Kox, E. Stavitski, J.C. Groen, J. Pérez-Ramírez, F. Kapteijn, B.M. Weckhuysen, Chem. Eur. J. 14 (2008) 1718.

[32] S.J. Reitmeier, O.C. Gobin, A. Jentys, J.A. Lercher, Angew. Chem. Int. Ed., 48 (2009) 533.

[33] B.C. Lippens, J.H. de Boer, J. Catal., 4 (1965) 319.

[34] S. Brunauer, P.H. Emmett, E. Teller, J. Am. Chem. Soc. 60 (1938) 309.

[35] E.P. Barrett, L.G. Joyner, P.P. Halenda, J. Am. Chem. Soc., 73 (1951) 373.

[36] J. Sirita, S. Phanichphant, F.C. Meunier, Anal. Chem., 79 (2007) 3912.

[37] F.C. Meunier, A. Goguet, S. Shekhtman, D. Rooney, H. Daly, Appl. Catal. A, 340 (2008) 196.

[38] P.B. Weisz, Ind. Eng. Chem. Res., 34 (1995) 2692.

[39] S.F. Garcia, P.B. Weisz, J. Catal., 121 (1990) 294.

[40] F.C. Meunier, L. Domokos, K. Seshan, J.A. Lercher, J. Catal., 211 (2002) 366.

[41] J.C. Groen, L.A.A. Peffer, J.A. Moulijn, J. Pérez-Ramírez, Colloid Surface A, 241 (2004) 53.

[42] J.C. Groen, J.A. Moulijn, J. Pérez-Ramírez, Ind. Eng. Chem. Res., 46 (2007) 4193.

[43] Q. Huang, H. Vinh-Thang, A. Malekian, M. Eic, D. Trong-On, S. Kaliaguine, Microporous Mesoporous Mater., 87 (2006) 224.

[44] F. Eder, J.A. Lercher, Zeolites, 18 (1997) 75.

[45] If one of two crystals with identical pore structure and dimension would adsorbed ten times more molecules, then the corresponding desorption slope would be typically 10-fold lower.

[46] O.C. Gobin, S.J. Reitmeier, A. Jentys, J.A. Lercher, J. Phys. Chem. C, 113 (2009) 20435.

[47] C. Mondelli, V. Dal Santo, A. Trovarelli, M. Boaro, A. Fusi, R. Psaro, S. Recchia, Catal. Today, 113 (2006) 81.

[48] J. Kärger, S. Vasenkov, Microporous Mesoporous Mater., 85 (2005) 195.

[49] W.O. Haag, R.M. Lago, P.B. Weisz, Faraday Discuss. Chem. Soc., 72 (1981) 317.

[50] N.Y. Chen, T.F. Degnan, C. Morris Smith, Molecular Transport and Reaction in Zeolites: Design and Application of Shape Selective Catalysis, John Wiley & Sons Inc., 1994.

503 [51] D.M. Ruthven, M.F.M. Post, in: H. van Bekkum, E.M. Flanigen, J.C. Jansen
504 (Eds.), Introduction to Zeolite Science and Practice, vol. 137, Elsevier,
505 Amsterdam, 2001, pp. 525-578.
506 [52] S. van Donk, A. Broersma, O.L.J. Gijzeman, J.A. van Bokhoven, J.H. Bitter, K.P.
507 de Jong, J. Catal., 204 (2001) 272.
508

Table 1. Composition and porosity of the H-ZSM-5 samples.

Sample	Si/Al[a] / mol mol^{-1}	V_{pore}[b] / cm^3 g^{-1}	V_{micro}[c] / cm^3 g^{-1}	V_{meso}[d] / cm^3 g^{-1}	S_{meso}[c] / m^2 g^{-1}	S_{BET}[e] / m^2 g^{-1}
SP	47	0.27	0.17	0.10	62	457
SAT	33	0.58	0.13	0.45	250	578
LP	30	0.15	0.14	0.01	5	350
LAT	24	0.28	0.12	0.16	120	415

[a] ICP-OES.

[b] Volume of N_2 adsorbed at $p/p_0 = 0.99$.

[c] *t*-plot.

[d] $V_{meso} = V_{pore} - V_{micro}$.

[e] BET method.

Figure captions

Figure 1. N_2 isotherms at 77 K and the thereof derived BJH adsorption pore size distributions (insets) for the parent small (SP, ▲) and large (LP, ●) H-ZSM-5 crystals and the corresponding small (SAT, △) and large (LAT, ○) samples in mesoporous form.

Figure 2. DRIFTS spectra collected over the H-ZSM-5 crystals at 428 K. (a) SP and SAT under Ar or at equilibrium under 178 Pa of *o*-xylene, (b) SP and SAT under Ar or at equilibrium under 1 kPa isooctane and (c) LP and LAT under Ar and at equilibrium under 1 kPa isooctane.

Figure 3. Desorption of *o*-xylene and isooctane at 428 K from the commercial H-ZSM-5 sample in parent (SP, ▲) and mesoporous (SAT, △) forms.

Figure 4. Desorption of isooctane at 428 K from the small and large H-ZSM-5 crystals in parent and mesoporous forms.

Figure 5. Equilibrium concentration of isooctane at 428 K over the H-ZSM-5 samples under 1 kPa of isooctane (solid bars). The corresponding accumulation factor, i.e. the ratio of isooctane concentration in the sample to that in the gas phase, is also shown (open bars).

550 Figure 1.

551

552

553

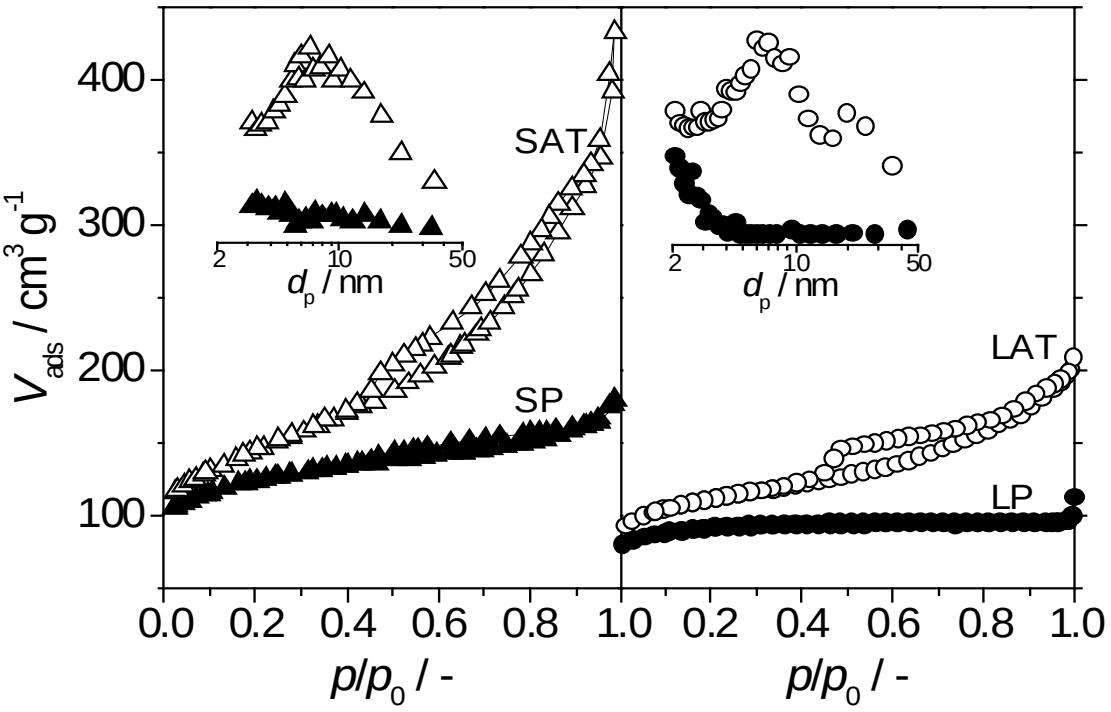

554

555 Figure 2.

556

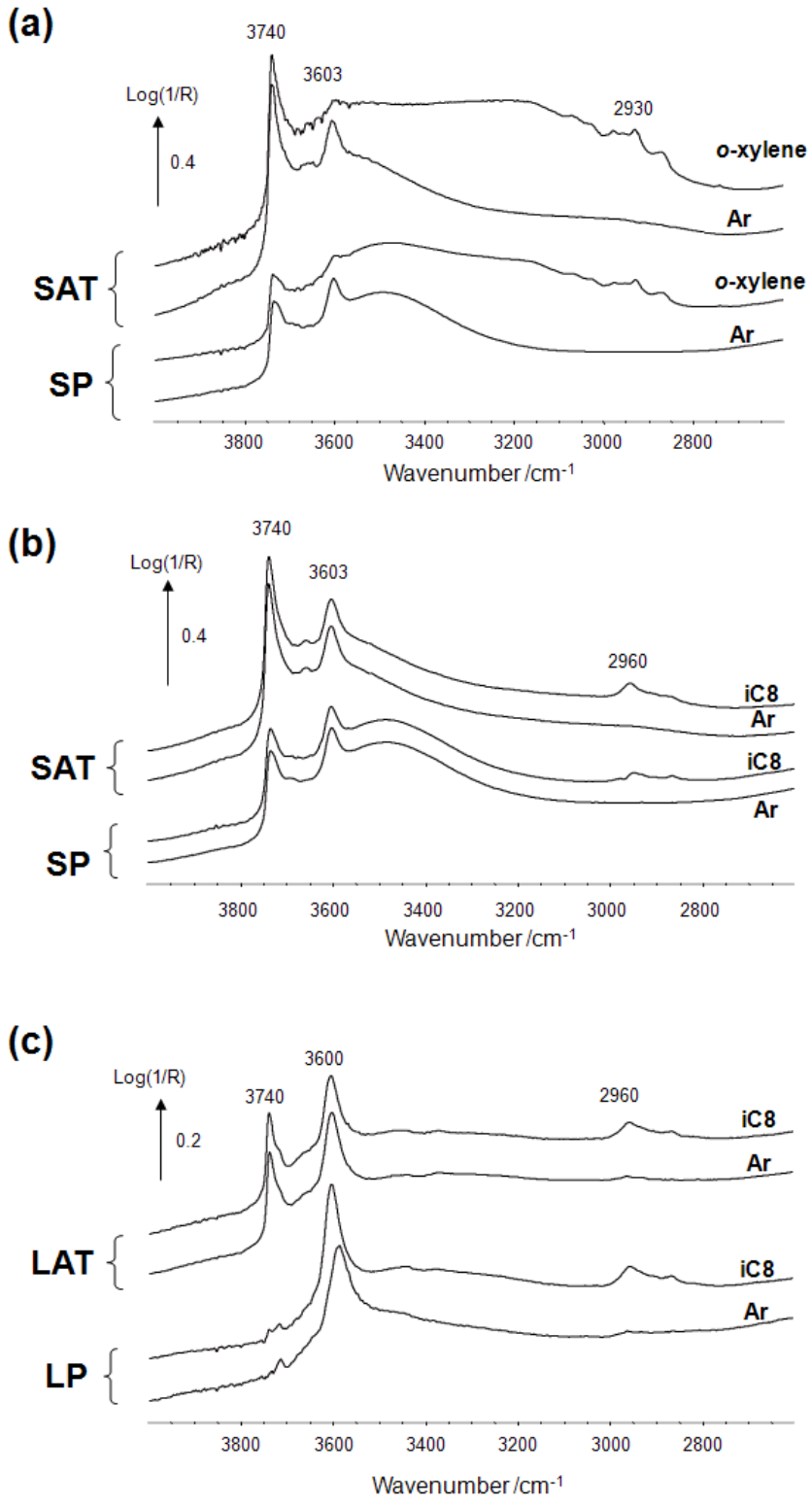

557

558

559 Figure 3.

560

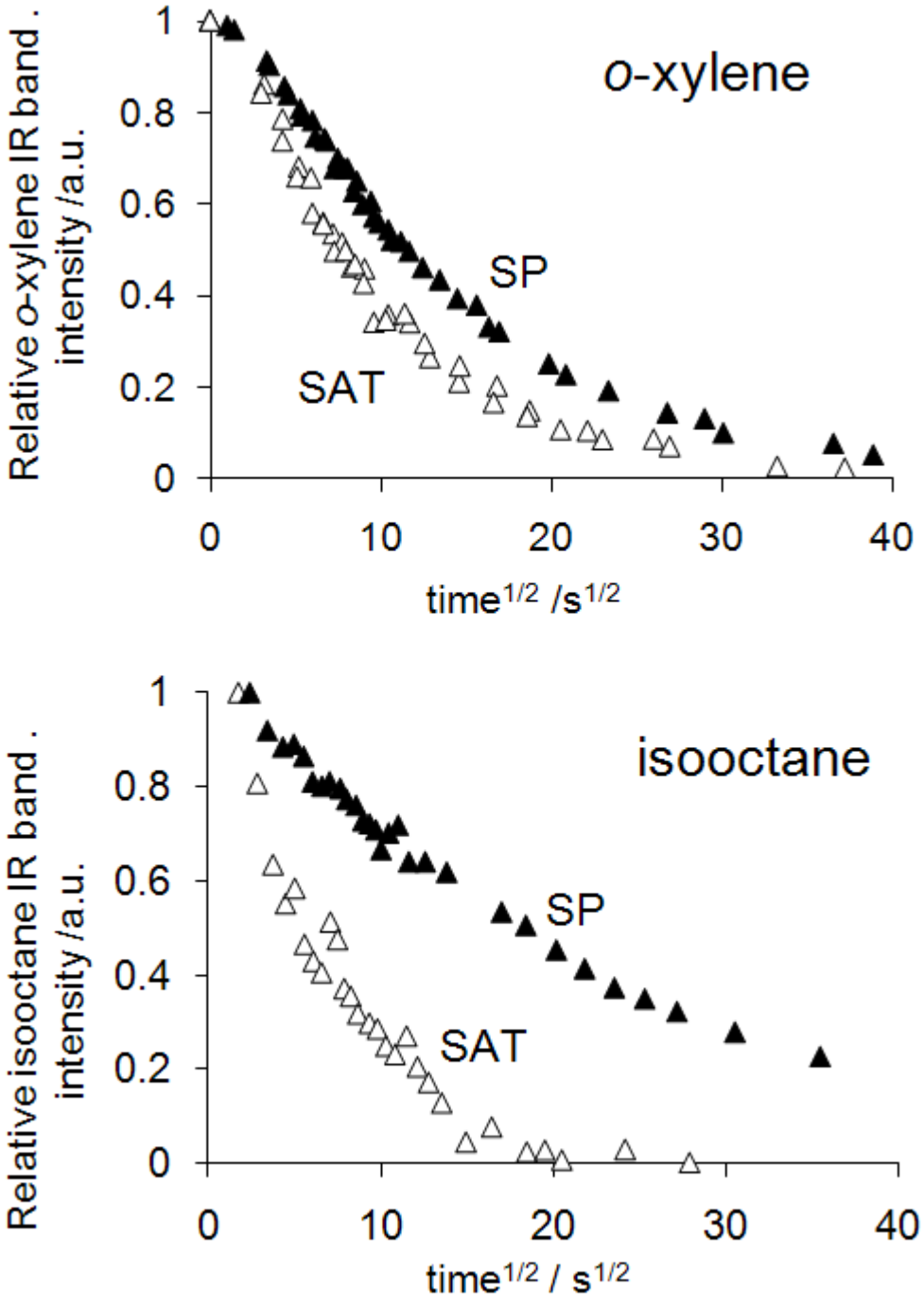

561

562

563 Figure 4.

564

565

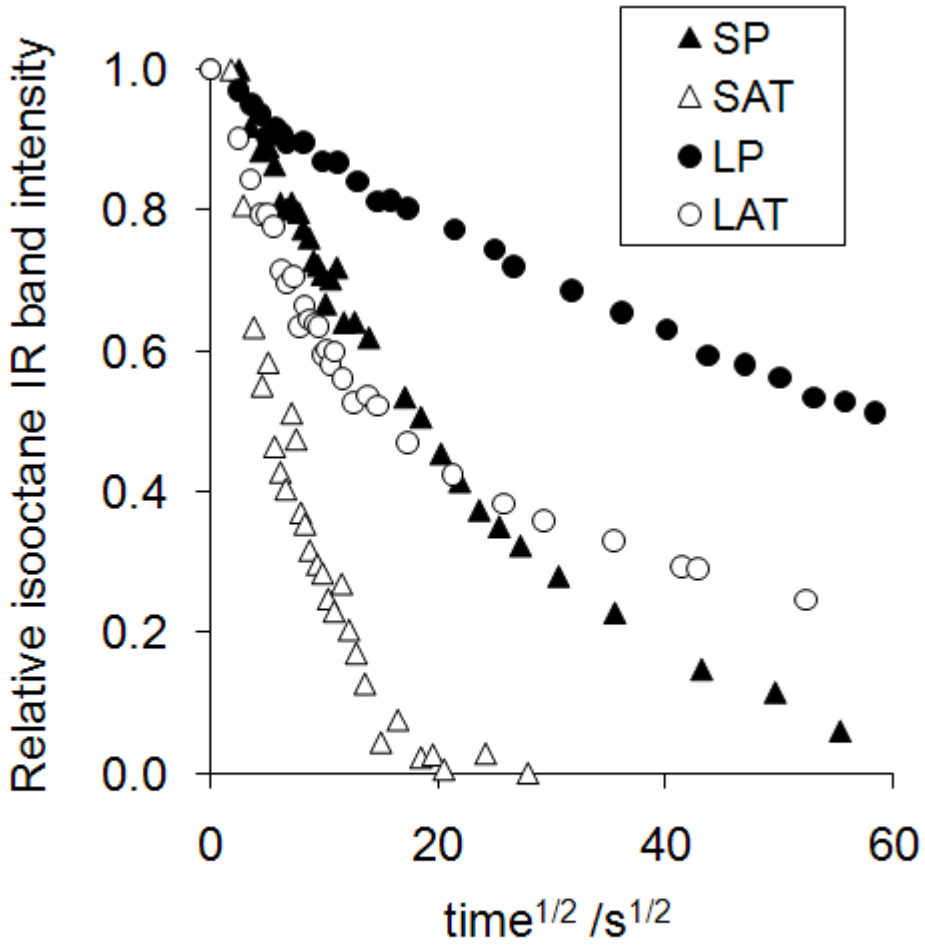

566

567 Figure 5.

568

569

570

571

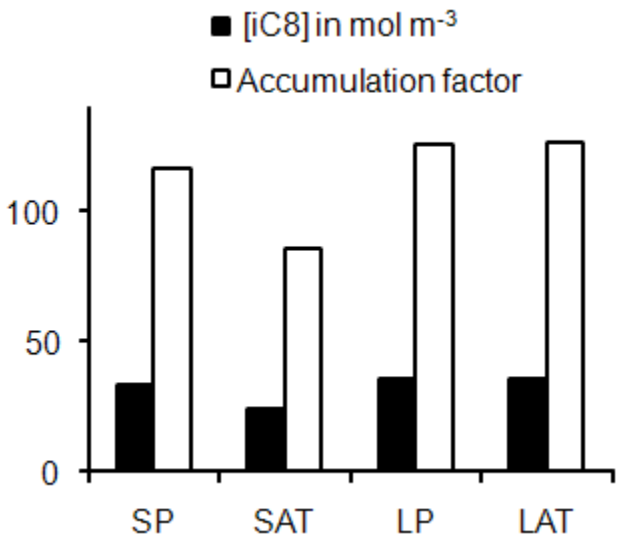

572